Supplemental Information

Cul4A-DDB1-mediated monoubiquitination of phosphoglycerate dehydrogenase promotes colorectal cancer metastasis via increased S-adenosylmethionine

Yajuan Zhang[1,8], Hua Yu[1,8], Jie Zhang[2,8], Hong Gao[1], Siyao Wang[1], Shuxian Li[2], Ping Wei[3], Ji Liang[1], Guanzhen Yu[4], Xiongjun Wang[5*], Xinxiang Li[6*], Dawei Li[6*], Weiwei Yang[1,7,9*]

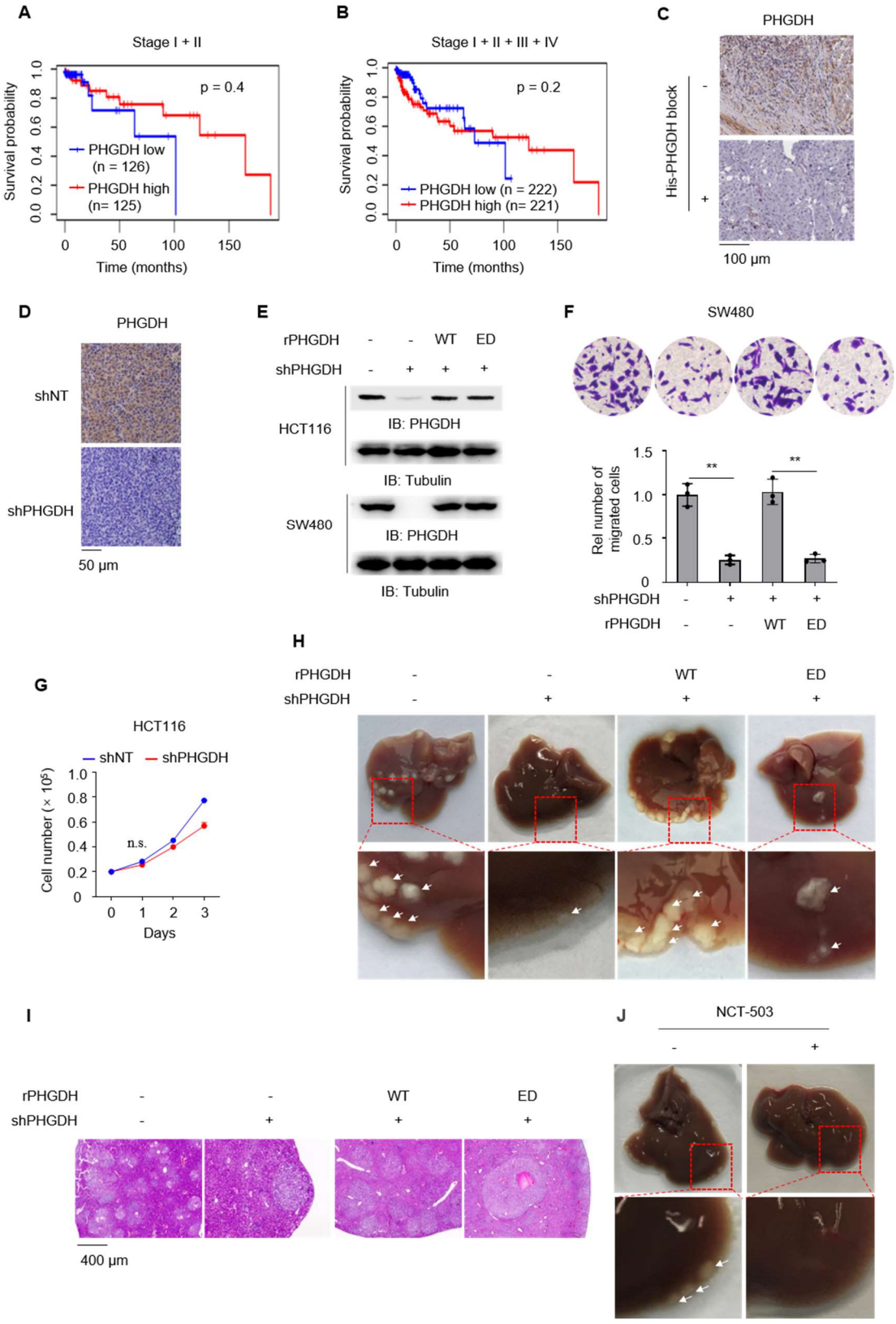
A
Stage I + II
Survival probability
p = 0.4
PHGDH low (n = 126)
PHGDH high (n= 125)
Time (months)
B
Stage I + II + III + IV
p = 0.2
PHGDH low (n = 222)
PHGDH high (n= 221)
C
PHGDH
His-PHGDH block
100 μm
D
PHGDH
shNT
shPHGDH
50 μm
E
rPHGDH
shPHGDH
HCT116
IB: PHGDH
IB: Tubulin
SW480
F
SW480
Rel number of migrated cells
G
HCT116
shNT
shPHGDH
Cell number (× 10⁵)
n.s.
Days
H
I
400 μm
J
NCT-503

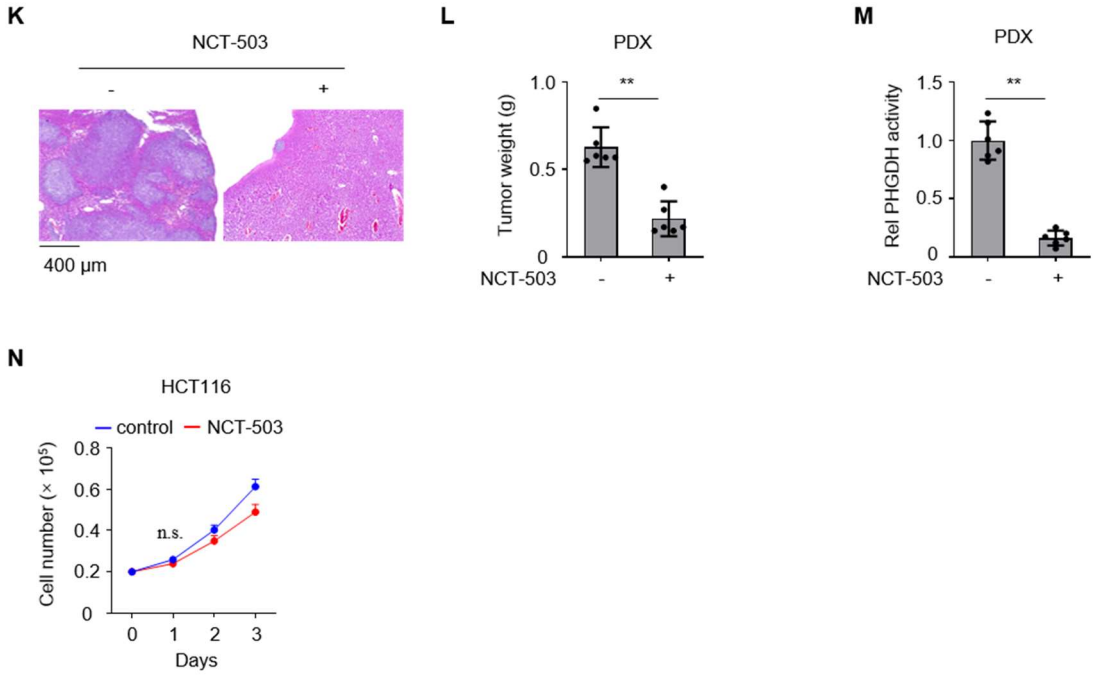

Figure S1. PHGDH Activity is important for CRC Metastasis. Related to Figure 1.

(F, G, N) Data represent the mean ± SD of three biologically independent experiments. F, 1-way ANOVA with Tukey's multiple comparison test; G, N, two-tailed Student's t-test.

(A, B) TCGA RNA-sequencing data of patients with colon adenocarcinoma were analyzed. Survival durations of 251 patients with colon adenocarcinoma with low or high expression of *PHGDH* were compared (A). Survival durations of 443 patients with colon adenocarcinoma with low or high expression of *PHGDH* were compared (B). Kaplan-Meier Method.

(C) Validation of antibody specificity. IHC analyses of human CRC specimens were performed with anti-PHGDH antibody in the absence or presence of His-PHGDH blocking protein. Data are representative of three biologically independent experiments.

(D) HCT116 cells expressing shNT or shPHGDH were subcutaneously implanted into BALB/c nude mice. IHC analyses were performed in dissected tumor tissues.

(E) HCT116 or SW480 cells stably expressing shRNA targeting shNT or PHGDH were infected with the lentivirus expressing rPHGDH WT or ED.

(F) SW480 cells stably expressing shNT or shPHGDH were infected with the lentivirus expressing rPHGDH WT or ED. Transwell migration assays were performed in these cells. Rel: relative.

(G) Cell proliferation was examined in HCT116 cells stably expressing shNT or shPHGDH.

(H, I) HCT116 cells stably expressing shNT or shPHGDH were infected with the lentivirus expressing rPHGDH WT or ED. Cells were injected into spleen of randomized BALB/c nude mice. Representative images of liver metastasis were shown (H). The metastatic nodules in the livers were dissected and stained with H&E. Representative images of H&E-stained metastatic nodules were shown (I).

(J, K) The metastatic tumor tissues were dissected from CRC patients with liver metastasis and subcutaneously implanted into randomized BALB/c nude mice. Mice were treated with or without NCT-503. Representative images of liver metastasis were shown (J). The metastatic nodules in the livers were dissected and stained with H&E. Representative images of H&E-stained metastatic nodules were shown (K).

(L, M) The metastatic tumor tissues were dissected from CRC patients with liver metastasis and subcutaneously implanted into randomized BALB/c nude mice. Mice were treated with or without NCT-503. 5 weeks after inoculation, the weights of dissected subcutaneous tumors were measured (L). PHGDH activity in the tumors was determined (M).

(N) Cell proliferation was examined in HCT116 cells treated with or without 10 μM NCT-503.

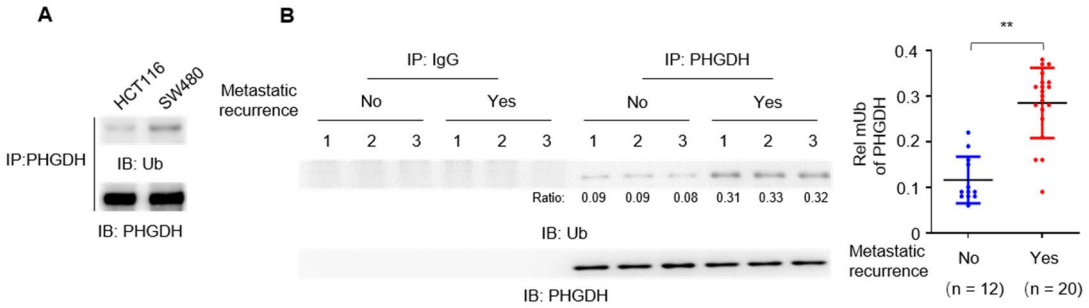

C

	Scan	Method	Score	m/z	Gene name
Ub-K21	1765	ITMS; CID	39.4	771.44 z=2	PHGDH
		GlyGlyK I L Q D G G L Q V V E K			
Ub-K33	2208	ITMS; CID	57.6	707.40 z=2	PHGDH
		I L Q D G G L Q V V E GlyGlyK			
Ub-K69	2753	ITMS; CID	30.8	949.53 z=2	PHGDH
		V T A D V I N A A E GlyGlyK L Q V V G R			
Ub-K129	2526	ITMS; CID	48.4	745.38 z=2	PHGDH
		Q I P Q A T A S M GlyGlyK D G K			
Ub-K146	3271	ITMS; CID	92.8	664.72 z=3	PHGDH
		F M G T E L N G GlyGlyK T L G I L G L G R			

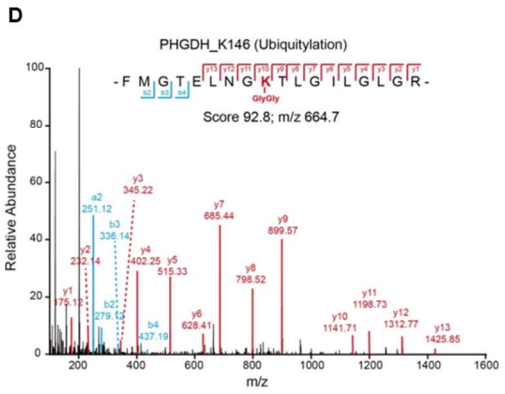

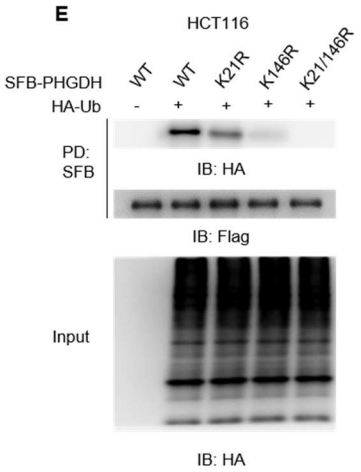

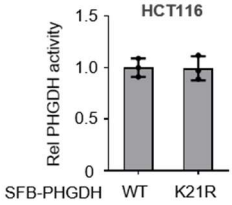

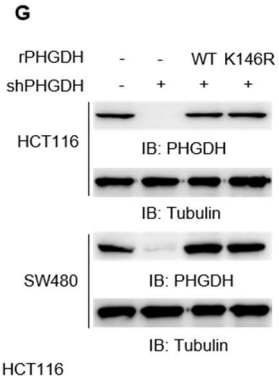

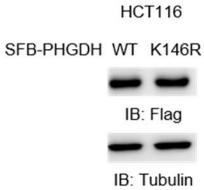

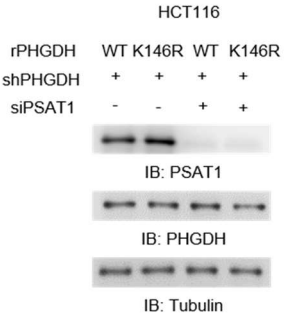

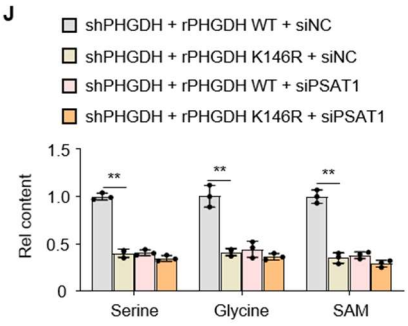

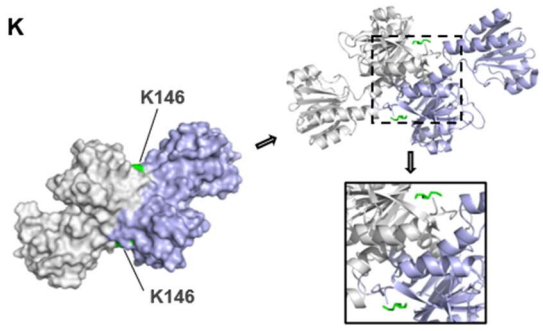

L

Protein IDs	Protein names	Intensity
O43175	PHGDH	344080000
V9HW96	CCT8	84988000
A0A140VJJ2	ESD	32022000
Q15785	TOM34	26397000
P31689	DNAJA1	20487000
A0A1B0GVH5	FTO	10028000
Q6UXS9	CASP12	7720700
Q59EJ3	HSP70	6386200
V9HWB8	PKM	4701500
Q13546	RIPK1	3127200

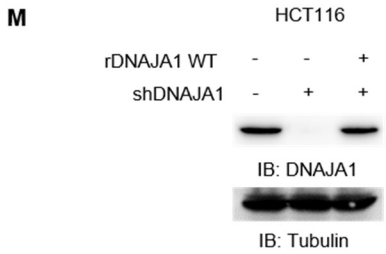

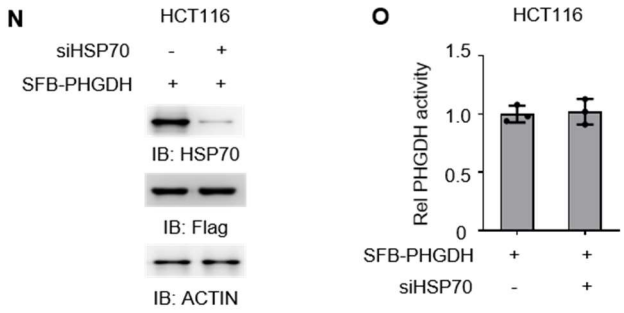

48

49 **Figure S2. Monoubiquitination Increases PHGDH Activity through DNAJA1-Dependent**

50 **PHGDH Tetrameric Formation.** Related to Figure 2.

51 (F, J, O) Data represent the mean ± SD of three biologically independent experiments

52 (two-tailed Student's t-test).

53 (A) HCT116 or SW480 cells were harvested and PHGDH proteins were immunoprecipitated

54 using anti-PHGDH antibody. IP: immunoprecipitation.

55 (B) PHGDH proteins were immunoprecipitated from primary tumors from CRC patients with

56 or without metastatic recurrence using anti-PHGDH antibody. We adjusted the amount of

57 immunoprecipitated PHGDH from the tumors of these two groups to the similar levels.

Monoubiquitination of PHGDH was examined using immunoblotting analyses with anti-ubiquitin antibody. Left, representative images of immunoblotting were shown. Right, semi-quantitative scoring was carried out. Data represent the mean ± SD (two-tailed Student's t-test). mUb, monoubiquitination.

(C-D) SFB-PHGDH was pulldown from HCT116 cells. The ubiquitinated residues in PHGDH, identified by mass spectrometry analyses, were listed (C). The mass spectrum of ubiquitinated K146 was presented (D).

(E) HCT116 cells stably expressing SFB-PHGDH WT or indicated mutants were transfected with or without HA-Ub.

(F) SFB-PHGDH proteins were pulldown from HCT116 cells stably expressing SFB-PHGDH WT or K21R with streptavidin agarose beads. PHGDH activity was determined.

(G) HCT116 or SW480 cells were depleted of endogenous PHGDH and rescued with rPHGDH WT or K146R.

(H) HCT116 cells were transfected with SFB-PHGDH WT or K146R.

(I, J) PHGDH-depleted HCT116 cells rescued with rPHGDH WT or K146R cells were transfected with siNC or siPSAT1. Immunoblotting analyses were performed in these cells (I). Cells were harvested for the measurement of intracellular serine, glycine and SAM (J).

(K) Structure of dimeric PHGDH was shown (PDB: 2G76). Green residue represents PHGDH K146.

(L) Mass spectrometry analyses of PHGDH-associated proteins were performed in HCT116 cells. The top 9 proteins that showed strong interactions with PHGDH were listed.

(M) HCT116 cells stably expressing SFB-PHGDH and shNT or shDNAJA1 were infected

with the lentivirus expressing EV or rDNAJA1 WT.

(N, O) HCT116 cells stably expressing SFB-PHGDH were transfected with siNC or siHSP70. Immunoblotting analyses were performed in these cells (N). PHGDH activity was measured in these cells (O).

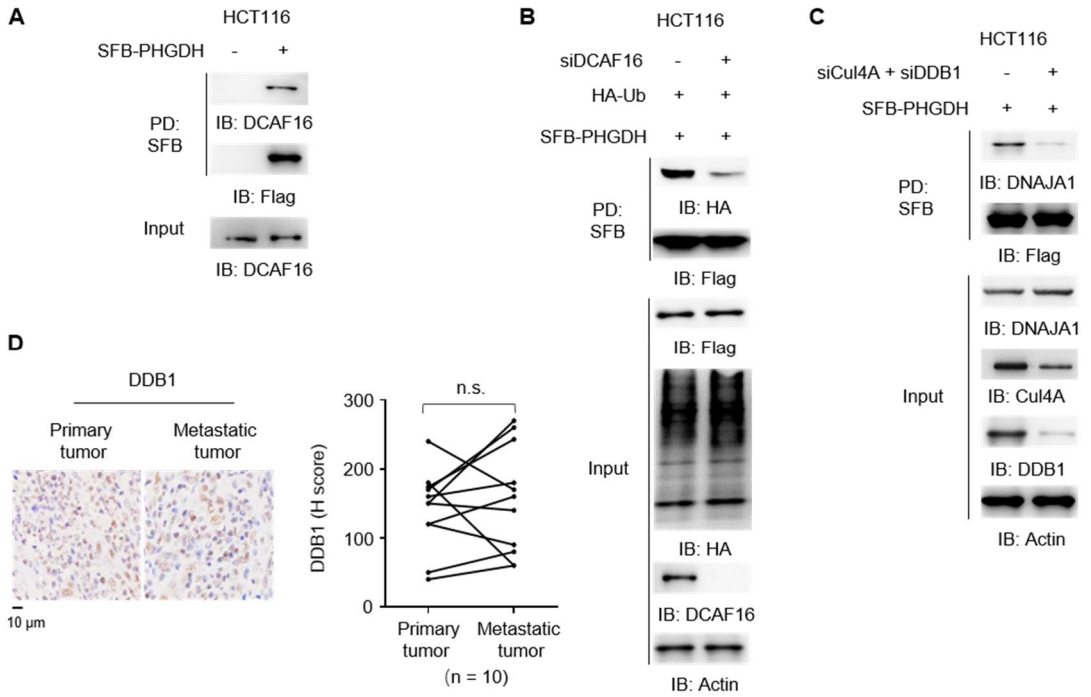

Figure S3. Cul4A-DDB1-DCAF16 Complex Mediates the monoubiquitination of PHGDH. Related to Figure 3.

(A) HCT116 cells were transfected with EV or SFB-PHGDH. SFB-PHGDH proteins were pulldown with streptavidin agarose beads.

(B) HCT116 cells stably expressing SFB-PHGDH were transfected with siNC or siDCAF16 and HA-Ub. SFB-PHGDH proteins were immunoprecipitated.

(C) HCT116 cells stably expressing SFB-PHGDH were transfected with siNC or siCul4A and siDDB1. SFB-PHGDH proteins were pulldown with streptavidin agarose beads.

(D) IHC staining was performed in paired primary tumors and hepatic metastatic tumors from 10 CRC patients using anti-DDB1 antibody. Staining scores of DDB1 were compared between primary tumors and metastatic tumors. Left, representative images of IHC staining were shown. Right, semi-quantitative scoring was carried out (paired t test, two-tailed).

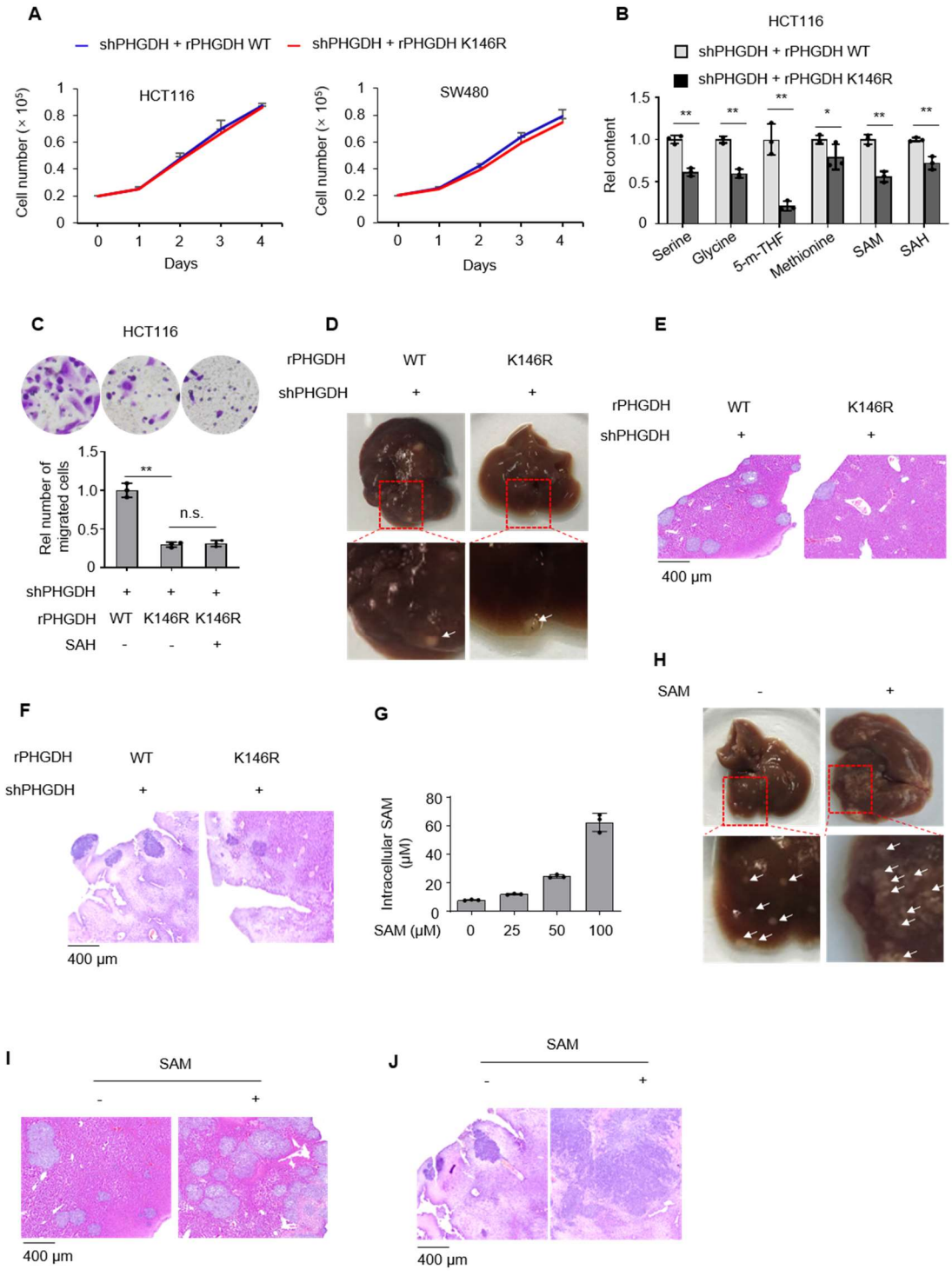

Figure S4. Increased SAM Levels by PHGDH K146mUb Promotes CRC Metastasis. Related to Figure 4.

(A, B, C, G) Data represent the mean ± SD of three biologically independent experiments A, B, two-tailed Student's t-test; C, 1-way ANOVA with Tukey's multiple comparison test.

(A) Cell proliferation was examined in PHGDH-depleted HCT116 or SW480 cells rescued with rPHGDH WT or K146R.

(B) PHGDH-depleted HCT116 cells were rescued with rPHGDH WT or K146R. Targeted metabolomics were performed to determine the intermediate levels of serine and glycine biosynthesis pathway and one-carbon metabolism.

(C) HCT116 cells were depleted of endogenous PHGDH and rescued with rPHGDH WT or K146R. These cells were supplemented with or without SAH (25 μM). Transwell migration assays were performed in these cells.

(D-E) Cells in (C) were injected into spleen of randomized BALB/c nude mice. Representative images of liver metastasis were shown (D). The metastatic nodules in the livers were dissected and stained with H&E. Representative images of H&E-stained metastatic nodules were shown (E).

(F) Luciferase-expressing PHGDH-depleted HCT116 cells rescued with rPHGDH WT or K146R were implanted into cecum of randomized BALB/c nude mice (six mice per group). 8 weeks after the implantation, H&E staining was performed in the dissected liver tissues from the mice. Representative images of H&E-stained metastatic nodules were shown.

(G) HCT116 cell were treated with increasing doses of SAM and intracellular SAM levels were examined.

(H-I) HCT116 cells were injected into spleen of randomized BALB/c nude mice (six mice per group), followed by the administration of SAM (20 mg/kg body weight) via oral gavage once daily for 3 weeks. 4 weeks after the injection, mouse livers were dissected. Representative images of liver metastasis were shown (H). The metastatic nodules in the livers were

127 dissected and stained with H&E. Representative images of H&E-stained metastatic nodules
128 were shown (I).
129 (J) Luciferase-expressing HCT116 cells were implanted into cecum of randomized BALB/c
130 nude mice (six mice per group). 2 weeks after the implantation, these mice were administrated
131 with SAM (20 mg/kg body weight) via oral gavage once daily for 4 weeks. 8 weeks after the
132 injection, H&E staining was performed in the dissected liver tissues from the mice.
133 Representative images of H&E-stained metastatic nodules were shown.
134

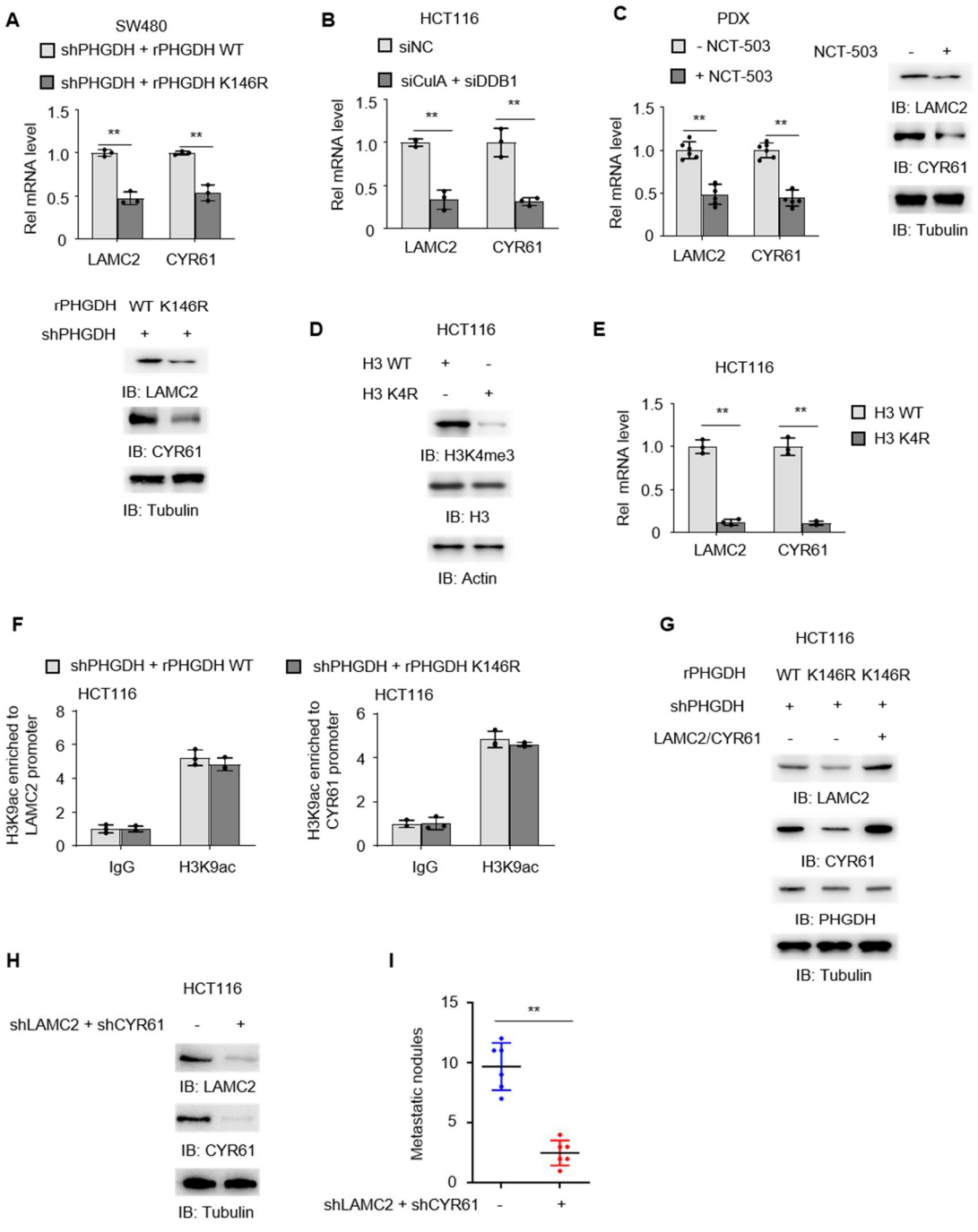

135

136 **Figure S5. PHGDH K146mUb Upregulates Cell Adhesion Gene Expression and**

137 **Promotes Tumor Cell Migration.** Related to Figure 5.

138 (A, B, E, F) Data represent the mean ± SD of three biologically independent experiments

139 (two-tailed Student's t-test).

140 (A) The mRNA levels (top) and protein levels (bottom) of *LAMC2* and *CYR61* were examined

in PHGDH-depleted SW480 cells rescued with rPHGDH WT or K146R.

(B) HCT116 cells transfected with siNC or siCul4A and siDDB1 were harvested and the mRNA levels of *LAMC2* and *CYR61* were examined.

(C) The metastatic tumor tissues were dissected from CRC patients with liver metastasis and subcutaneously implanted into randomized BALB/c nude mice (six mice per group). 1 week after the implantation, these mice were intraperitoneally injected with PHGDH inhibitor (NCT-503, 25 mg/kg body weight) once daily for 3 weeks. 5 weeks after inoculation, mice were euthanized. The mRNA levels (top) and protein levels (bottom) of *LAMC2* and *CYR61* were examined in dissected tumor nodules. Data represent the mean ± SD of mRNA level per mouse in six mice (two-tailed Student's t-test).

(D, E) HCT116 cells were transfected with H3 WT or H3 K4R. Immunoblotting analyses were performed (D). The mRNA levels of *LAMC2* and *CYR61* were examined in these cells (E).

(F) PHGDH-depleted HCT116 cells were rescued with rPHGDH WT or K146R. ChIP analyses were performed with anti-acetylated H3K9 (H3K9ac) antibody.

(G) PHGDH-depleted HCT116 cells rescued with rPHGDH WT or K146R were infected with or without the lentivirus expressing both LAMC2 and CYR61.

(H, I) HCT116 cells were infected with the lentivirus expressing shNT or shLAMC2 and shCYR61. Immunoblotting analyses were performed (H). Cells were injected into spleen of randomized BALB/c nude mice (six mice per group). 4 weeks after the injection, mouse livers were dissected. The metastatic nodules in the livers were counted and statistically analyzed (I). Data represent the mean ± SD of the metastatic nodules per mouse in six mice

(two-tailed Student’s t-test).

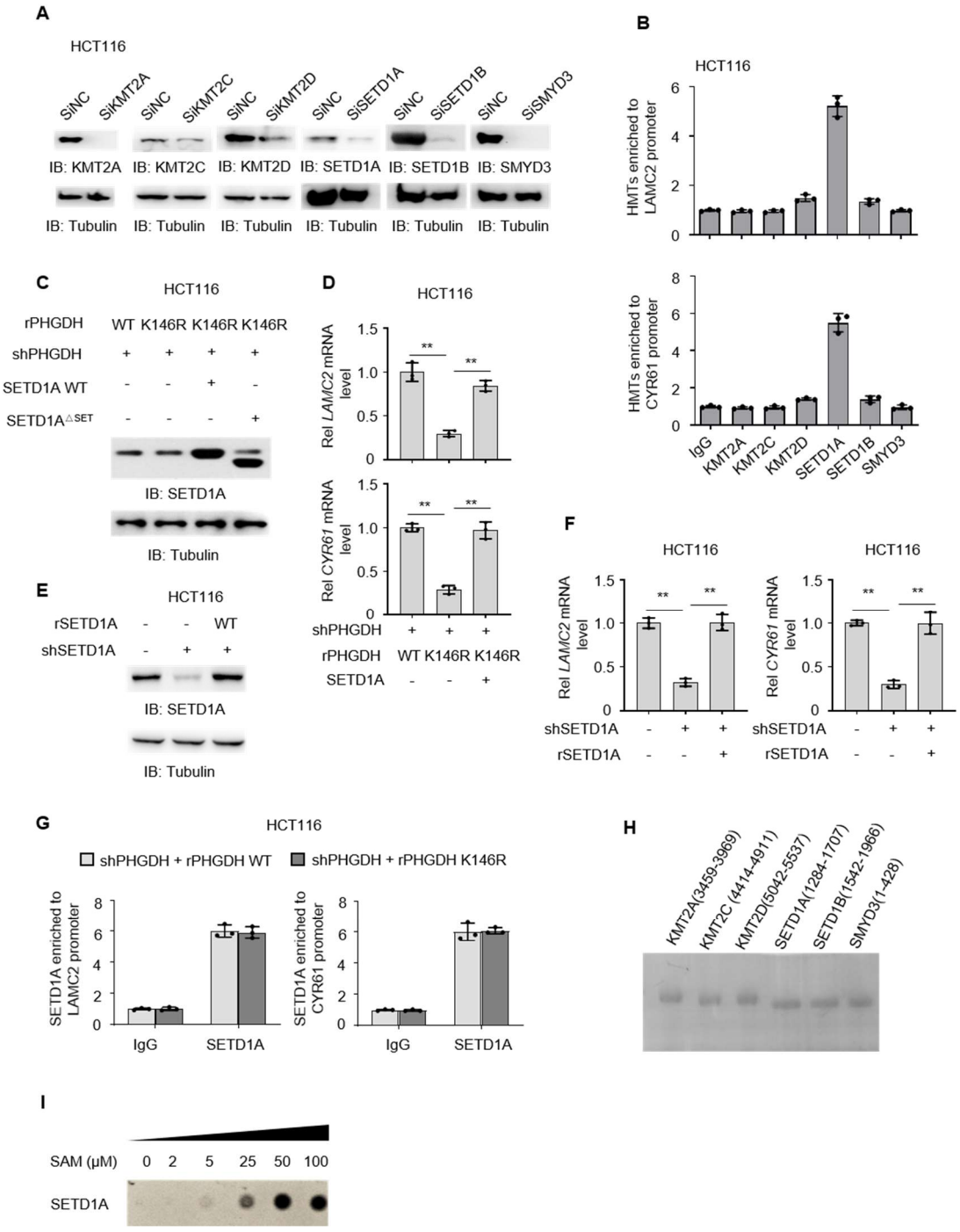

Figure S6. Increased SAM Levels by PHGDH K146mUb Promotes Tumor Cell Migration by Initiating SETD1A-Mediated Histone Methylation of *LAMC2* and *CYR61*.

Related to Figure 6.

(B, D, F, G) Data represent the mean ± SD of three biologically independent experiments D, F, 1-way ANOVA with Tukey's multiple comparison test; G, two-tailed Student's t-test.

(A) HCT116 cells were transfected with siRNAs targeting NC, KMT2A, KMT2C, KMT2D, SETD1A, SETD1B or SMYD3.

(B) ChIP analyses were performed in HCT116 cells with indicated antibodies.

(C) PHGDH-depleted HCT116 cells rescued with rPHGDH WT or K146R were infected with or without the lentivirus expressing SETD1A WT or SETD1A$^{\triangle SET}$. SETD1A expression was examined by immunoblotting analyses.

(D) PHGDH-depleted HCT116 cells rescued with rPHGDH WT or K146R were infected with or without the lentivirus expressing SETD1A. The mRNA levels of *LAMC2* and *CYR61* were examined.

(E, F) HCT116 cells were depleted of endogenous SETD1A and rescued with rSETD1A. SETD1A expression was examined by immunoblotting analyses (E). The mRNA levels of *LAMC2* and *CYR61* were examined (F).

(G) ChIP analyses with anti-SETD1A antibody were performed in PHGDH-depleted HCT116 cells rescued with rPHGDH WT or K146R.

(H) Recombinant methyltransferase domain of KMT2A, KMT2C, KMT2D, SETD1A, SETD1B and SMYD3 were purified from bacteria and stained with Coomassie Blue.

(I) In vitro methylation assays were performed with purified recombinant His-tagged methyltransferase domains of SETD1A, SAM and H3K4 peptide, followed by dot blot analysis with anti-H3K4me3 antibody.